Photo-crystallography: from the structure towards the electron density of metastable states

V. Legrand, Chiara Carbonera, Sébastien Pillet, Mohamed Souhassou, Jean-François Létard, Philippe Guionneau, Claude Lecomte

Photo-crystallography : from the structure towards the electron density of metastable states.

V Legrand[1], C Carbonera[2], S Pillet[1], M Souhassou[1], J F Létard[2], P Guionneau[2] and C Lecomte[1]

[1] Laboratoire de Cristallographie et de Modélisation des Matériaux Minéraux et Biologiques, CNRS UMR 7036, UHP Nancy 1, Faculté des sciences, Boulevard des Aiguillettes, BP 239, 54506 Vandoeuvre-lès-Nancy Cédex, France.

[2] Institut de Chimie de la Matière Condensée de Bordeaux, UPR CNRS 9048, Université de Bordeaux 1, Groupe de Sciences Moléculaires, 87 Avenue du Docteur Schweitzer, 33608 Pessac cedex, France.

Abstract. A photo-crystallographic study of $Fe(btr)_2(NCS)_2.H_2O$ was performed in order to describe the modification of structures and charge densities on going from the ground low spin (LS) state to the metastable high spin (HS) state during the LIESST phenomenon at 15K. Related photo-magnetic and spectroscopic measurements are also described. We show that at 15K, the thermally quenched and photo-induced structures of the metastable HS state are identical. For comparison, we also derived the structure of the HS and LS states at 130K in the hysteresis loop; the thermal spin transition and the LIESST spin transition exhibit similar structural behaviours.

1. Introduction

Spin crossover compounds are particularly interesting owing to their bistability properties; they are very promising for their possible use as thermal switches, display devices or data storage elements [1]. $3d^4$ to $3d^7$ transition metal ions in octahedral environment may exhibit different spin states (high spin (HS), low spin (LS)) depending on the crystal field. If the crystal field effect is of the order of the electron pairing energy, a spin transition may occur with a variation of the external conditions [2]. At very low temperature, for some of these coordination compounds, a metastable state can be obtained under light irradiation [3]: the LIESST effect (Light Induced Excited Spin State Trapping) is a reversible phenomenon [4] and can only be induced below a limit temperature (T_{LIESST}) [5; 6].

$Fe(btr)_2(NCS)_2.H_2O$ (btr=4,4'-bis-1,2,4-triazole) is the archetype of highly cooperative spin crossover complexes. It exhibits abrupt thermal spin transitions (123.5K and 144.5K in the cooling (HS → LS) and warming (LS → HS) modes respectively) with a 21K hysteresis loop. The complex crystallizes in space group C2/c without any symmetry change during the spin transition; the crystal structure has previously been described in the HS state at 293K [7] and in the LS state at 104K [8]. The central iron is coordinated to four btr groups, which act as bidendate ligands, leading to a 2D layer architecture perpendicular to the crystallographic *a* axis. The coordination sphere is completed by two

thiocyanate anions in axial position almost perpendicular to the 2D layers. Figure 1 represents the molecular and crystal structure in the HS state.

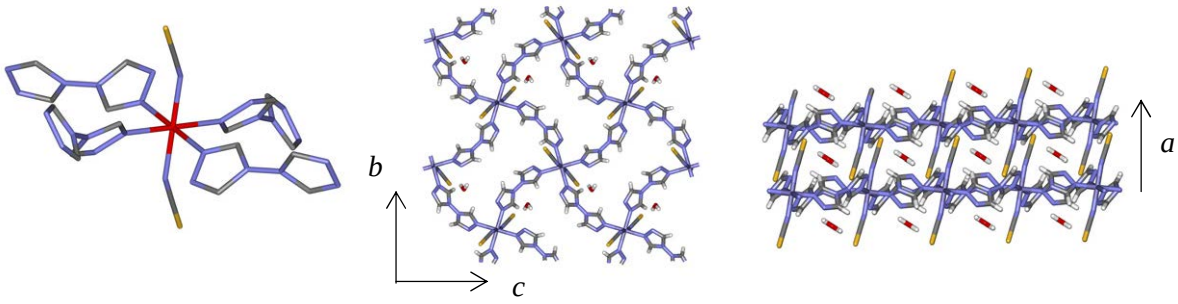

Figure 1. Molecular, layer and crystal structure of $Fe(btr)_2(NCS)_2.H_2O$.

The goal of this crystallographic and photo-crystallographic study is to better understand the solid state physical behaviours occurring during the LIESST and the thermal spin transitions. We aim also at deriving and characterizing for the first time the electron density distribution of a light induced excited state in spin crossover materials. Pioneering work in this field has been performed by Coppens *et al.* on linkage isomerism of nitrosyl iron complexes [9].

2. Experimental details

The btr ligand and its iron complex $Fe(btr)_2(NCS)_2.H_2O$ were synthesized as previously described [10]. Single crystals, suitable for accurate crystallographic studies, were grown by slow solvent evaporation in aqueous solution. The selected crystals were embodied in vacuum grease and mounted on glass fibre, in order to keep the crystals intact upon passing the spin transition [8]. The diffraction data were collected using an Oxford Diffraction Xcalibur diffractometer with Mo(Kα) radiation, equipped with a CCD detector; at 15K and 130K the cooling systems were an Oxford Diffraction He open flow Helijet and an N_2 open flow cryostream respectively. Collected data were integrated using software CRYSALIS and averaged using SORTAV [11]. An analytical absorption correction was applied (μ = 1.018 mm^{-1}) (using CRYSALIS) and the absorption due to the grease was corrected with SORTAV. The structures were solved by direct methods and refined using SHELX [12].

Table 1. Crystal parameters and labelling of the measured spin states at 15K and 130K.

15 K	**LS (1)**	**HS (2) Photo-induced**	**HS (3) Quenched**
a (Å)	11.1626(4)	10.874(2)	10.9047(5)
b (Å)	12.5839(6)	13.063(2)	13.1125(1)
c (Å)	12.7543(6)	13.147(2)	13.162(1)
β (°)	92.284(3)	90.83(1)	90.883(8)
130 K	**LS (4)**	**HS (5)**	
a (Å)	11.1971(8)	10.9580(5)	
b (Å)	12.5847(9)	13.1506(4)	
c (Å)	12.7567(9)	13.1551(6)	
β (°)	92.307(6)	91.151(4)	

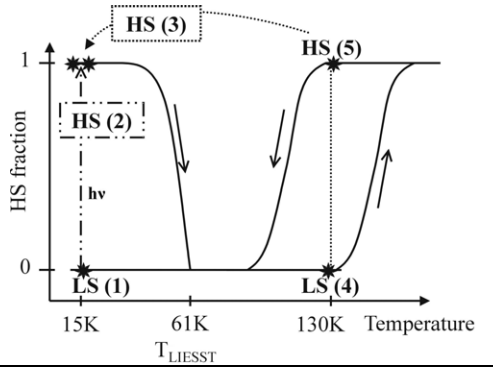

High resolution accurate X-ray diffraction data have been collected on $Fe(btr)_2(NCS)_2.H_2O$ at 15K on the LS(1) and metastable HS(2; 3) states according to [13]; a data collection was also performed in the hysteresis loop at 130K in both LS(4) and HS(5) states. Table 1 gives the crystal parameters in the different studied spin states, the inserted figure displays the spin transition properties and spin state

labelling. The metastable HS state was generated in two ways: by optical Ar-Kr laser excitation through the LIESST effect (HS(2)) (λ = 488 nm; P = 50 mW; exposure time = 30 s), and by thermal quenching (HS(3)) (using a flash cooling of the single crystal sample on the diffractometer).

Spectroscopic measurements were performed by optical reflectivity from room temperature to 10K in the visible range. A probe light of 400 to 900 nm, generated by a lamp was focussed on a powder sample; the reflected beam was analysed using a spectrophotometer. Magnetic susceptibility measurements were carried out using a MPMS-55 Quantum Design SQUID magnetometer equipped with an optical fibre allowing the illumination of the sample.

3. Results and discussion

3.1. Spectroscopic and photo-magnetic measurements

The absorption spectra of $Fe(btr)_2(NCS)_2.H_2O$ have been measured as a function of temperature by reflectivity. Figure 2 shows the absorption spectra attributed to the HS (160 K), LS (100 K) and metastable photo-induced HS (10 K) states of the complex on cooling and heating modes. All LS spectra show a band at about 550 nm (ν ~ 18200 cm^{-1}) which could be attributed to the $^1A_1 \rightarrow {}^1T_1$ transition according to the Tanabe-Sugano diagram [14] for an ion with a d^6 electronic configuration in an octahedral ligand field. For crystallographic experiments, we chose the excitation wavelength λ = 488 nm to ensure a high light penetration and to initiate the light induced LS → HS conversion (LIESST effect) below the LIESST temperature. We also measured a band with a maximum around 875 nm (ν ~ 11400 cm^{-1}) corresponding to the $^5T_2 \rightarrow {}^5E$ transition of the molecules in the HS state; to initiate the light induced HS → LS conversion we used the excitation wavelength λ = 830 nm at 10 K and we observed the Reverse-LIESST effect by magnetic measurement.

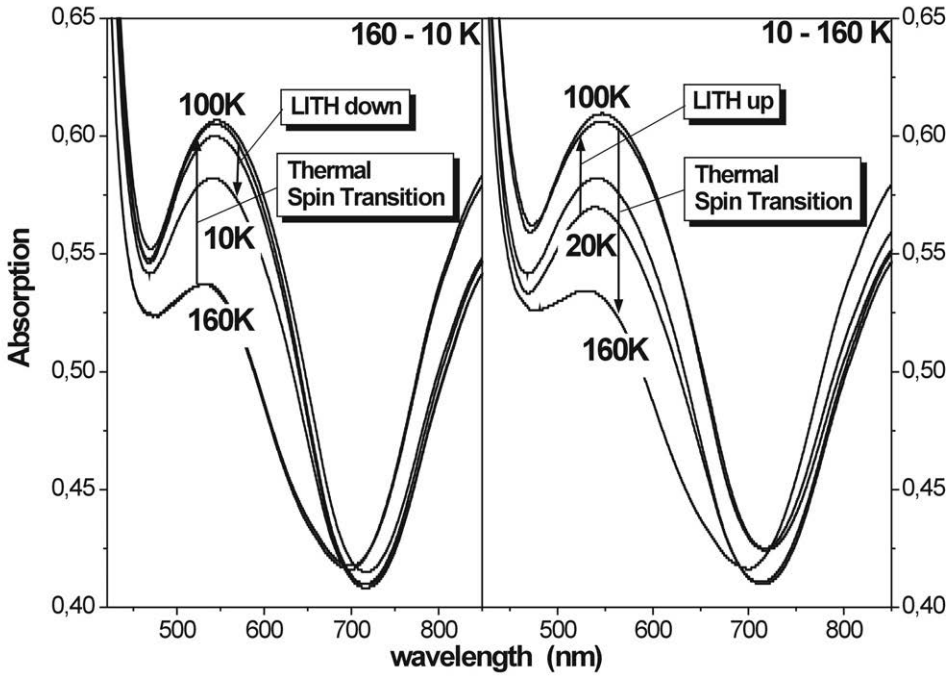

Figure 2. Reflectivity spectra at selected temperatures, on cooling (left) and heating (right) modes.

To complete the spectroscopic study and to better understand the excitation and relaxation processes, photo-magnetic measurements have been undertaken as a function of temperature and time. Two measurements were made. First, the sample was cooled down to 10K and irradiated at 514 nm and 5 mW/cm^2. After 27 hours excitation, a quantitative conversion of nearly 33% ($\chi_M T$ ~ 1.2

$cm^3.K.mol^{-1}$) was observed (figure 3). Then from this obtained photo-induced partial HS state, the temperature was increased till the LIESST HS to LS relaxation occurred at T_{LIESST} = 52K.

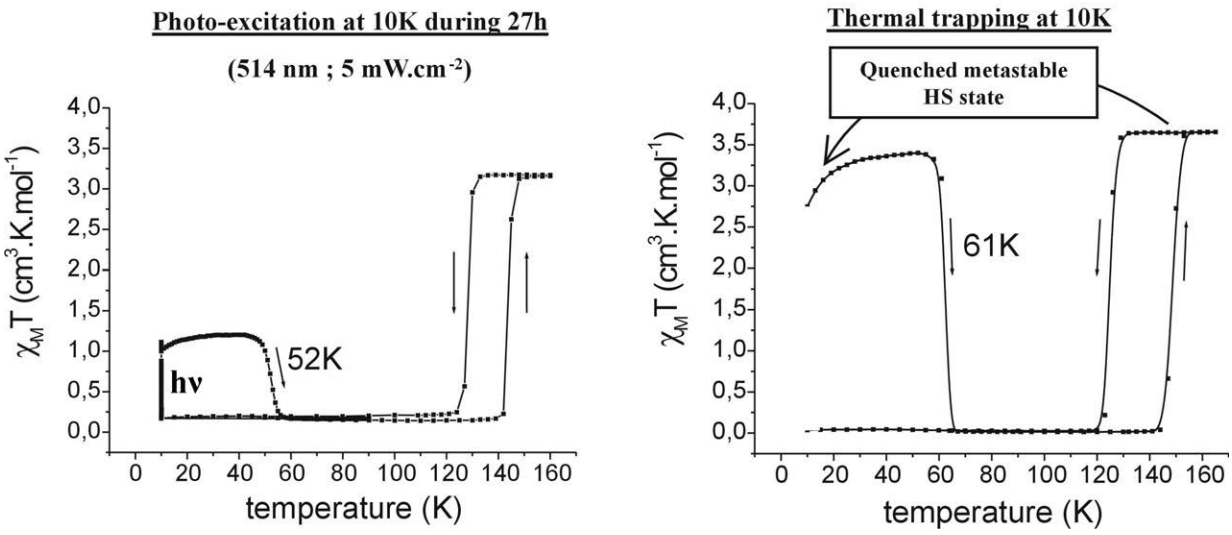

Figure 3. Photo-magnetic measurements of $Fe(btr)_2(NCS)_2.H_2O$: photo-induced (left) and quenched (right) HS states.

For the second magnetic measurement, the sample was rapidly quenched to 10K within 60 s. A nearly 100 % metastable state ($\chi_M T$ ~ 2.8 $cm^3.K.mol^{-1}$) was thus generated at 10K; by increasing the temperature, the limit HS to LS relaxation temperature was determined at T_{LIESST} = 61K (figure 3). Finally, the relaxation of the complex was checked and found to be very slow at 15K: the HS-fraction decreased by about 1% in 10 hours. These last data are crucial for photo-crystallographic experiments; they prove that at sufficiently low temperature, the HS to LS relaxation is slow enough to allow a complete diffraction experiment to be performed on a metastable stationary state.

3.2. Crystal Structures

As written above the structure of $Fe(btr)_2(NCS)_2.H_2O$ was refined in 5 distinct states (table 1) in order to describe the effects of the LIESST and thermal transitions on the structure, in particular to compare both photo-excited and thermally trapped HS structures.

The variation of the lattice parameters versus temperature is shown in figure 4; for the HS state, a thermal contraction of the *a* and *b* parameters and a thermal expansion of the *c* parameter is observed, this behaviour is the same for the LS state. The thermal evolution of the lattice parameters for the thermal HS state and the metastable HS state follows the same trend with a general linear dependence over the whole temperature range. During the HS → LS thermal transition, an increase of the *a* parameter is measured, related to a realignment of the NCS ligands which moves away the 2D layers stack along the *a* axis. A decrease of the *b* and *c* parameters, related to the contraction of the coordination sphere during the spin transition and a shortening of the Fe-N bonds, is also observed.

From the thermal evolution of the lattice parameters, the thermal deformation tensor has been calculated. It is related to the internal stresses and gives information about the strength of the intermolecular interactions in the crystal. A high value of the tensor means large changes of the lattice parameters related to weak interactions; on the contrary, a small value of the tensor indicates little changes of the lattice parameters owing to strong interactions. The diagonalized forms of the LS and HS thermal deformation tensors are shown in table 2, the eigenvectors are also mentioned. We see that the principal directions of the interactions are nearly the crystallographic axis, especially in the LS state. The tensor coefficients show that the strongest interactions lie in the *b*-*c* plane, which is related

to the high cooperativity of the 2D layer structure. The thermal deformation tensor also indicates the smallest interactions in the *a* direction which is the direction of the layer stacking with weak Van der Waals interactions.

Table 2. Diagonalized forms of the LS (left) and HS (right) thermal deformation tensor (ε_{LS} and ε_{HS}) with the associated eigenvectors (M_{LS} and M_{HS}). Cartesian axis basis: $\vec{e}_2 // \vec{b}^*$; $\vec{e}_3 // \vec{c}^*$; $\vec{e}_1 // (\vec{e}_2 \wedge \vec{e}_3)$.

$\varepsilon_{LS} = \begin{pmatrix} 50.5 & 0 & 0 \\ 0 & 20.8 & 0 \\ 0 & 0 & -20.8 \end{pmatrix}$	$\varepsilon_{HS} = \begin{pmatrix} 97.3 & 0 & 0 \\ 0 & 26.2 & 0 \\ 0 & 0 & -14.5 \end{pmatrix}$
$M_{LS} = \begin{pmatrix} 1 & 0 & \approx 0 \\ 0 & 1 & 0 \\ \approx 0 & 0 & 1 \end{pmatrix}$	$M_{HS} = \begin{pmatrix} 1 & 0 & 0.29 \\ 0 & 1 & 0 \\ -0.29 & 0 & 1 \end{pmatrix}$

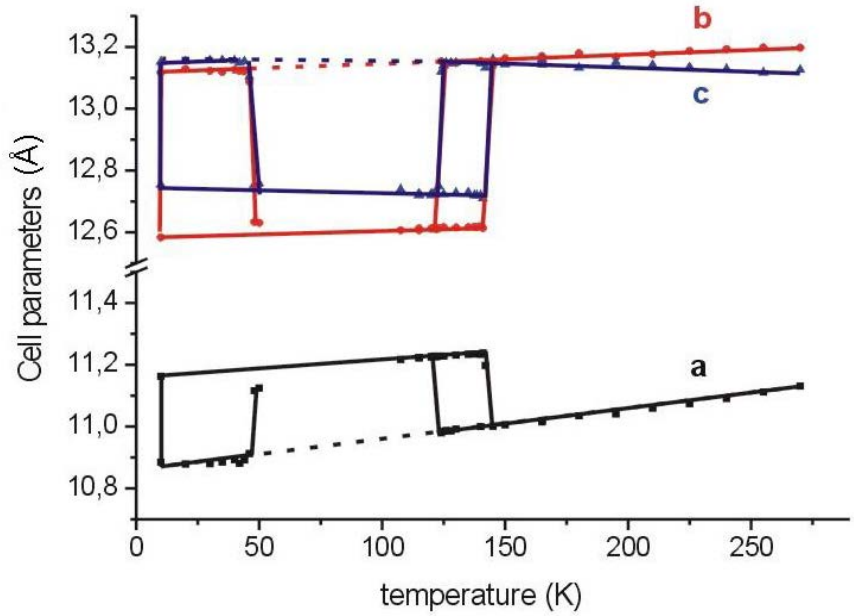

Figure 4. Evolution of the lattice parameters.

During the LS → HS LIESST transition (15K, 488 nm, 40 mW), we also followed the evolution of the diffraction patterns versus time and observed a Bragg peak splitting, which is characteristic of the growth of HS phase domains as already noticed during the thermal transition [8]. The conversion was nearly achieved within 15min [15].

Let's compare the two structures of the metastable HS state at 15K obtained either by photo-excitation (HS(2)) or quenched by flash cooling (HS(3)). The Fe-N bond lengths are <d(Fe-N_{btr})> = 2.170(1)Å and d(Fe-N_{NCS}) = 2.134(1)Å and <d(Fe-N_{btr})> = 2.160(6)Å and d(Fe-N_{NCS}) = 2.129(4)Å for the trapped and photo-induced HS states respectively. The other bond lengths and angles are also equal within 3 sigma. Therefore the two experimental metastable HS structures are undistinguishable given the experimental accuracy.

Table 3. Geometric differences of the coordination sphere of the LS and HS for the LIESST transition (15 K) and the thermal transition (130 K). The variation of the coordination sphere parameters for the LIESST transition is shown on the attached figure.

	15K LIESST transition	130K thermal transition
bonds	**LS(1) – HS(3)**	**LS(4) – HS(5)**
Fe-N_{NCS} (Å)	+0.183(1)	+0.176(7)
<Fe-Nbtr> (Å)	+0.199(1)	+0.207(6)
N-C (Å)	+0.006(2)	+0.009(10)
C-S (Å)	-0.011(1)	-0.011(8)
angles	**LS(1) – HS(3)**	**LS(4) – HS(5)**
N1-Fe-N2	+0.64(5)°	+0.89(26)°
N1-Fe-N7	+0.01(5)°	-0.04(27)°
N2-Fe-N7	+0.17(5)°	+0.03(24)°
Fe-N1-C1	-13.4(1)°	-13.4(6)°

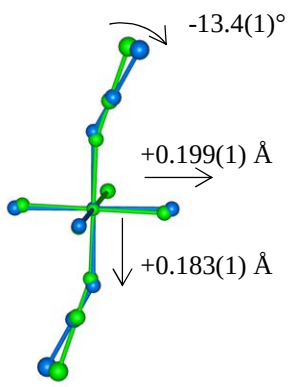

For spin transition compounds, it is commonly observed that the main structural variations occur in the coordination sphere [16]. During the LS → HS LIESST transition at 15K, the Fe-N bonds increase by $<\Delta d(Fe\text{-}N_{btr})>$ = +0.199(1)Å and $\Delta d(Fe\text{-}N_{NCS})$ = +0.183(1)Å with a change of -13.4(1)° in the alignment of the NCS ligand. Moreover, the distortion of the $Fe\text{-}N_6$ octahedron, as calculated by [17]: $\Sigma_{HS}^{trapped}$ = 16.6° and Σ_{LS} = 14.7°, is very small compared to other $Fe(L)_2(NCS)_2$ compounds ($<\Sigma_{HS}>_{28\ compounds}$ = 71°).

It is also interesting to compare the structural modifications attributed to the thermal transition to those occurring during the LIESST transition. The large thermal transition hysteresis allows to measure both states at exactly the same temperature which means that there is no thermal lattice contraction between the LS and HS states; the structural variations are only due to the spin transition. As shown on table 3 the LS-HS bond lengths and angles variations at the two temperatures are very close to each other; therefore the LIESST and thermal transitions lead to the same structural changes.

3.3. Electron density of the metastable state

The electron density modelling in $Fe(btr)_2(NCS)_2.H_2O$ is underway at 15K in the LS and metastable HS states, according to the Hansen-Coppens model [18], to characterize the interactions and determine the d-orbitals population. These results will be described in detail in a forthcoming paper. Figure 5 gives the experimental deformation electron density around the iron for both spin states as defined by:

$$\Delta\rho(\vec{r}) = \frac{1}{V}\sum_{\vec{H}}\left(\frac{1}{k}\left|F_{obs}(\vec{H})\right| - \left|F_{sph}(\vec{H})\right|\right)e^{i\Phi_{sph}}e^{-2i\pi\vec{H}\cdot\vec{r}}$$

where V is the unit cell volume, k the scale factor, $\vec{H}$ the scattering vector, F_{obs} and F_{sph} the observed and model structure factor amplitudes, Φ_{sph} is the phase calculated according to the spherical model.

The data are accurate enough to distinguish the electron spin state of both systems. The electron lone pair of the nitrogen atoms which coordinates the iron clearly shows up. In the LS state, negative deformation density along the Fe-N directions indicate an electron deficit in the dz^2 and $dx^2\text{-}y^2$ Fe-orbitals, the diagonal directions are more populated. On the contrary, the metastable HS state is characterized by a positive more isotropic deformation density with higher concentration in the directions of the ligands, corresponding to the dz^2 and $dx^2\text{-}y^2$ Fe-orbitals. These observations are consistent with the ligand field effects in such octahedral surrounding.

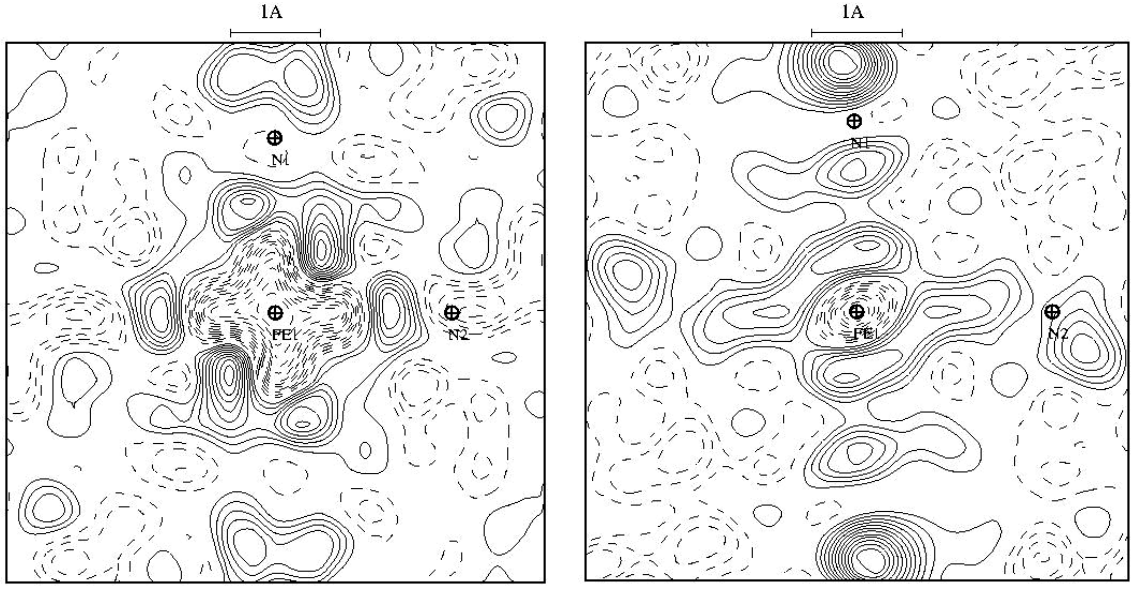

LS metastable HS

Figure 5. Deformation electron density map around the iron at 15K in the plane Fe-$N2_{btr}$-$N1_{NCS}$. $S < 0.7Å^{-1}$, $I > 3\sigma$, contour = $0.05e^{-}/Å^{3}$.

4. Conclusion

This paper describes for the first time the structural properties and preliminary charge density of an iron spin crossover compound during the thermal (130K) and the photo-excited (15K) transition processes. At 15K two HS states were accurately characterized, respectively obtained by photo-excitation and quenched from room temperature; the corresponding structures are the same within 0.01Å. The structural difference between the LS and HS phases at 15K (LIESST transition) and at 130K (thermal transition) was shown to be identical, in this well ordered system, within experimental accuracy. The data are accurate enough to derive the electronic properties of the compound and describe the d electron change upon the phase transition; the topology of the electron density and the bonding properties will be described in detail in a forthcoming paper.

Acknowledgements

The CNRS and the Université Henri Poincaré Nancy I are gratefully acknowledged for financial support. V L is indebted to the Ministère de l'éducation nationale, de l'enseignement supérieur et de la recherche for a doctoral fellowship.

References

[1] Kahn O, Kröber J and Jay C 1992 *Advanced Materials* **11** 718
[2] Gütlich P, Hauser A and Spiering H 1994 *Angew. Chem. Int. Ed. Engl*. **33** 2024
[3] Decurtins S, Gütlich P, Köhler C P and Spiering H 1984 *Chem. Phys. Lett*. **105** 1
[4] Hauser A 1986 *Chem. Phys. Letters* **124** 543
[5] Létard J F, Capes L, Chastanet G, Moliner N, Létard S, Real J A and Kahn O 1999 *Chem. Phys. Lett*. **313** 115
[6] Letard J F, Guionneau P, Nguyen O, Sanchez Costa J, Marcen S, Chastanet G, Marchivie M and Goux-Capes L 2005 *Chemistry - A European Journal* **000**
[7] Vreugdenhil W, Van Diemen J H, De Graaff R A G, Haasnoot J G, Reedijk J, Van der Kraan A M, Kahn O and Zarembowitch J 1990 *Polyhedron* **9** 2971

[8] Pillet S, Hubsch J and Lecomte C 2004 *Eur. Phys. J.* **B 38** 541
[9] Coppens P, Vorontsov I, Graber T, Gembicky M and Kovalevsky A 2005 *Acta Cryst*. **A 61** 162
[10] Vreugdenhil W, Gorter S, Haasnoot J G and Reedijk J 1985 *Polyhedron* **4** 1769
[11] Blessing R H 1995 *Acta. Cryst.* **A 51** 33
[12] Sheldrick G M 1997 *Shelx97. Program for the structure solution and refinement* (University of Gottingen, Germany)
[13] Legrand V, Pillet S, Souhassou M, Létard J F, Guionneau P and Lecomte C 2005 *J. Applied Cryst.* in submission
[14] Decurtins S, Gutlich P, Hasselbach K M, Hauser A and Spiering H 1985 *Inorg. Chem.* **24** 2174
[15] Lecomte C, Aubert E, Legrand V, Porcher F, Pillet S, Guillot B and Jelsch C 2005 *Z. Kristallogr.* **220** 373
[16] Marchivie M, Guionneau P, Létard J F and Chasseau D 2003 *Acta Cryst.* **B 59** 479
[17] Guionneau P, Brigouleix C, Barrans Y, Goeta A E, Létard J F, Howard J A K, Gaultier J and Chasseau D 2001 *C. R. Acad. Sci. Paris Chimie* **4** 161
[18] Hansen N K and Coppens P 1978 *Acta Cryst*. **A 34** 909